Analysis and Modeling of Dual-Band GSM Networks

Wai-Ru Lai, Yi-Bing Lin, and Herman Chung-Hwa Rao

Abstract: **This paper studies interconnection of DCS1800 and GSM900 dual-band networks. Two types of interconnection configurations for GSM services, non-overlap and overlap, are described. We propose analytic and simulation models to investigate the benefit of the overlap configuration. Our results explain how the radio channel capacities, the inter-system handoff failure rate, the originating call traffic ratio and the offered loads affect the system performance. This study indicates that with appropriate overlap configuration, the GSM dual-band network can significantly improve the quality of cellular service.**

Index Terms: **DCS1800, dual-band networks, GSM, interconnection.**

I. INTRODUCTION

Existing GSM networks operate at three frequency bands at 900 MHz, 1.8 GHz, and 1.9 GHz. The differences among these GSM networks are operating frequencies and power levels. They all utilize the same core GSM network following GSM MAP (Mobile Application Part) protocol [3]. To support roaming among GSM networks in different frequency bands, dual-band or triple-band GSM mobile stations (MSs) have been developed. In Taiwan, GSM900 (GSM service operated at 900 MHz) and DCS1800 (GSM service operated at 1800 MHz) licenses have been issued to several private cellular service providers. Two service providers, Tuntex Telecom and TransAsia, have GSM900 licenses. Three service providers, KG Telecom, MobiTai and Pacific Cellular, have DCS1800 licenses, where MobiTai has been merged into KG Telecom in 1999. Two service providers, Chunghwa Telecom and FarEastone, have both GSM900 and DCS1800 licenses. GSM base transceiver stations (BTSs) have been intensively deployed in Taiwan. Before January 1999, Chunghwa Telecom has deployed 2765 BTSs, FarEastone has deployed 2001 BTSs, and Pacific Cellular has deployed 2496 BTSs. These numbers continue to increase. Over 4 million customers have subscribed to the GSM services, and the service penetration rate is anticipated to grow.

One of the major GSM network issues in Taiwan is the interconnection of DCS1800 and GSM900 networks among various service providers, which is referred to as the heterogeneous PCS issue [11]. Interconnections of DCS1800 and GSM900 networks can be *non-overlap* or *overlap*. The non-overlap configuration extends the coverage area of the GSM services. On the other hand, the overlap configuration increases the radio channel capacity at the same service area. In this paper, we describe the non-overlap and the overlap configurations for GSM services. Then we propose analytic and simulation models to investigate the benefit of the overlap configuration. Our study indicates that with appropriate overlap configuration, the GSM dual-band network can significantly improve the quality of service by reducing the call incompletion probability.

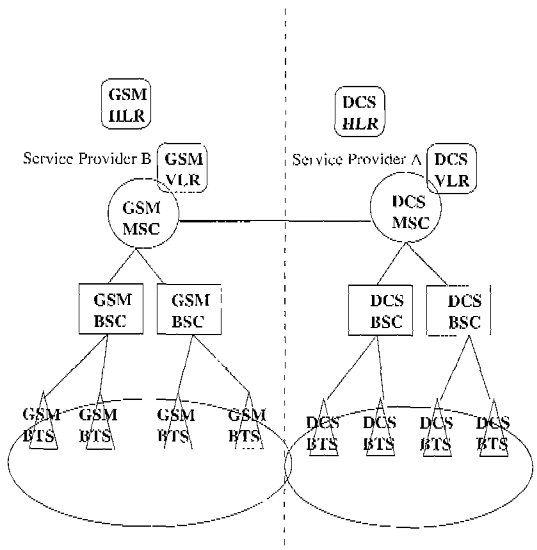

Fig. 1. Non-overlap dual-band GSM architecture.

We assume that the reader is familiar with the GSM terms such as home location register (HLR), visitor location register (VLR), base transceiver station (BTS), base station controller (BSC), base station (BS), mobile switching center (MSC), roaming and handoff. Details of these terms and GSM operations can be found in [3], [14], [9], [8], [17], [13].

II. NON-OVERLAP GSM CONFIGURATION

In Taiwan, non-overlap GSM configuration interconnects DCS1800 and GSM900 systems belonging to different service providers. The non-overlap architecture is illustrated in Fig. 1. Through roaming agreement, a customer of service provider A (DCS1800 service) can originate/terminate cellular calls at the service area of service provider B (GSM900 service) if the customer holds a dual-band MS. During a phone conversation, the customer can hand off from one network to another network through the inter-system handoff procedure. Fig. 2 illustrates the trunk connection before and after the inter-system handoff [9], where a BS represents of a BTS and a BSC. The new and old BSs are connected to two different MSCs. In this figure, a communicating GSM user moves out of the BS served by MSC A

Manuscript received March 30, 1999; approved for publication by Youngnam Han, Division II Editor, June 24, 1999.

Wai-Ru Lai and Yi-Bing Lin are with Department of Computer Science and Information Engineering, National Chiao Tung University, Hsinchu, Taiwan, R.O.C., e-mail: liny@csie.nctu.edu.tw.

Herman Chung-Hwa Rao is with AT&T Laboratories-Research, USA.

1229-2370/99/$10.00

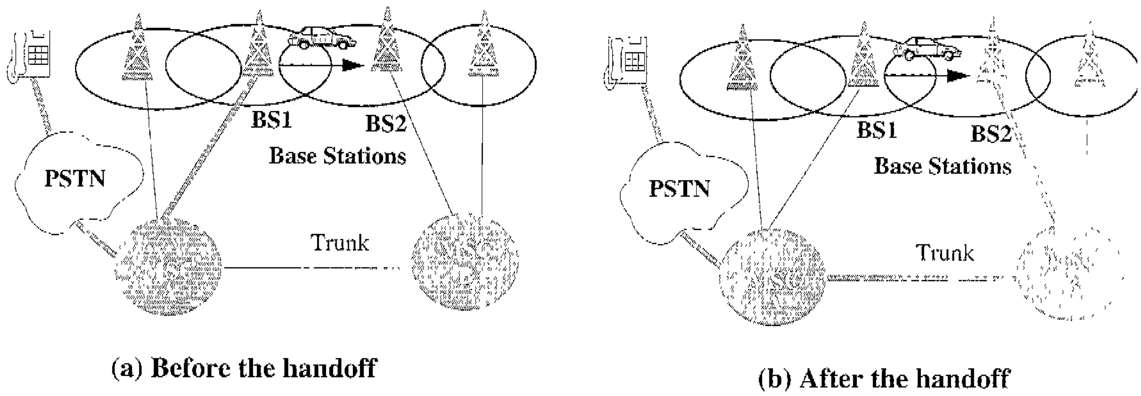

Fig. 2. Inter-system handoff.

and enters the area covered by MSC B. The inter-system handoff procedure is described in the following steps.

1. MSC A requests MSC B to perform handoff measurement. MSC B then selects a candidate BS for handoff. Suppose that the candidate BS2 is found. MSC B returns the signal quality parameter values and other information to MSC A.
2. MSC A checks if the MS has made too many handoffs or if inter-system trunks are not available. If so, MSC A exits the procedure. Otherwise, MSC A asks MSC B to set up a voice channel. Suppose that a voice channel is available in BS2. MSC B asks MSC A to start the radio link transfer.
3. MSC A sends the MS a handoff order. The MS tries to synchronize with BS2. After the MS is connected to BS2, MSC B informs MSC A that the handoff is successful. MSC A then connects the call path (trunk) to MSC B and completes the handoff procedure.

In this inter-system handoff process, MSC A is referred to as the *anchor MSC*, and is always in the call path (the thick links in Fig. 2) after the handoff. This anchor approach is selected for cellular systems because the re-establishment of a new call path (without involving MSC A) between MS and the new MSC will require extra trunk release/setup operations in Public Switched Telephone Network (PSTN), which is not available or is not cost effective.

We note that the inter-system handoff is an expensive operation. Besides the long handoff delay time, the failure rate of an inter-system handoff is typically more than 5 times of an inter-BTS handoff [15]. The failure is due to network response timeout or the lack of network resources such as inter-MSC trunk.

III. OVERLAP GSM CONFIGURATION

Unlike the non-overlap configuration, the overlap configuration allows a customer to select either DCS1800 service or GSM900 service at the same location. In Taiwan, this configuration interconnects DCS1800 and GSM900 systems belonging to the same service providers, and there are two different types of connections among the BTSs, BSCs and MSCs. These approaches are described below.

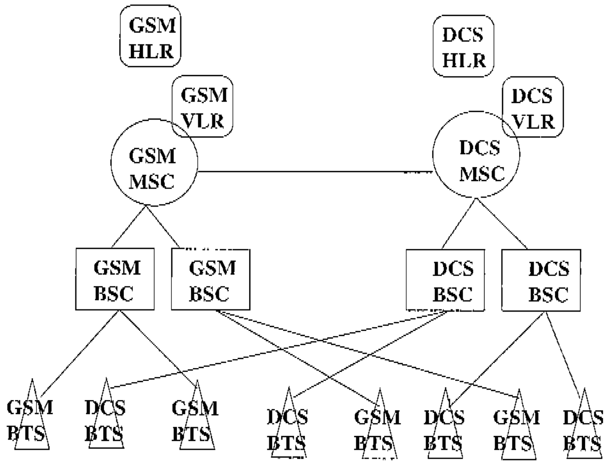

Fig. 3. Type-I overlap dual-band GSM architecture.

A. *Type-I Connection*

The overlap architecture for Type-I connection is illustrated in Fig. 3. This connection installs the BTSs of the DCS1800 and GSM900 networks at the same area, i.e., they are two independent networks operating at the same area. As we will show later, Type-I connection cannot utilize the radio channels efficiently. In Taiwan, this connection was deployed due to historical reason. The service provider first deployed and operated a GSM900 system. Later, the DCS1800 network was deployed as an independent network. Around late 1998, the service provider determined to merge the two networks. The resulting system consists of individual GSM networks where the DCS1800 and GSM900 BTSs are co-located at the same area. To share the radio capacities of DCS1800 and GSM900 BTSs in Type-I connection, modifications to the networks have been made:

- For call origination, a *directed-retry* technique is used to share the DCS1800 and GSM900 radio resources. Suppose that a dual-band MS registers at the DCS1800 VLR. To originate a call, the MS makes the call attempt through the DCS1800 BTS. If no idle channel is available in that BTS, then the DCS1800 network directs the MS to retry the GSM900 BTS. If an idle channel in the GSM900 BTS exists, then the MS originates the call

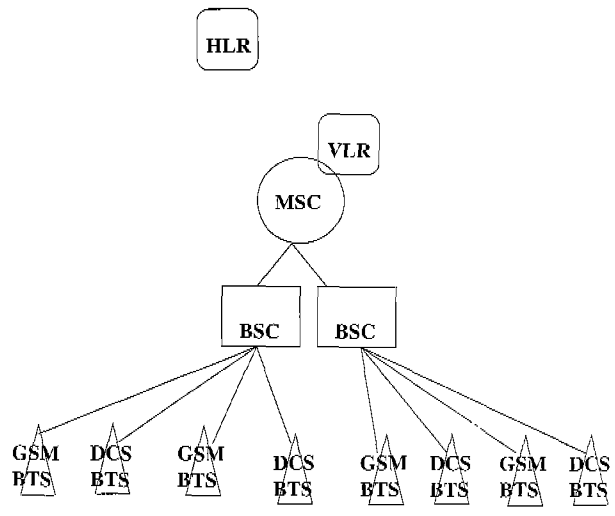

Fig. 4. Type-II overlap dual-band GSM architecture.

through the GSM900 network. Thus, the MS benefits from GSM900/DCS1800 radio resource sharing at the cost of a potential call retry.

- Like the systems in the non-overlap configuration, an inter-system handoff is required to support the inter-BTS handoff for adjacent DCS1800 and GSM1900 BTSs. As mentioned before, the cost for inter-system handoff is expensive and the failure rate is high.

For call termination, the dual-band network with Type-I connection does not offer any capacity benefit. Consider the scenario where an MS's home system is DCS1800 network, and it registers at a GSM900 VLR. For a call termination to the MS, the call is always directed from the DCS1800 HLR to the GSM900 MSC to page the MS. If the corresponding GSM900 BTS does not have any idle channel, the call is lost. Following the standard GSM call termination procedure[14], there is no way to re-direct the call through the DCS1800 MSC.

B. Type-II Connection

In Type-II connection, both GSM900 BTSs and DCS1800 BTSs are connected to the same BSC as shown in Fig. 4. Since there is only one HLR, the dual-band GSM configuration with Type-II connection can be considered as a single GSM network where the radio spectrum has been extended from one band to two bands. Furthermore, the co-siting arrangement is available. That is, the GSM900 and DCS1800 BTSs are located at the same site so that both BTSs may share cabinet, feeder and antenna. Co-siting allows transmission reuse and cost reduction for site research, site preparation and site rental. However, it also introduces disadvantages. For example, site positioning and full coverage may not be optimized.

Consider a dual-band MS tuned at the DCS1800 band. To originate a call, the MS uses the DCS1800 signaling channel (specifically, the SDCCH channel) to make the call attempt. If the DCS1800 BTS does not have any idle channel but the adjacent GSM900 BTS does, then the BSC uses the DCS1800 signaling channel to instruct the MS to tune to the GSM900 frequency. Thus, the MS moves to the GSM900 BTS to originate the call without a retry. For call termination, the BSC will ask both GSM900 and DCS1800 BTSs to page the MS. The MS will connect to the BTS with best idle traffic channel. Similarly, an MS can hand off between a GSM900 BTS and a DCS1800 BTS following the efficient inter-BTS handoff procedure (because both BTSs connected to the same BSC). In FarEastone dual-band system, 8% of handoff decisions are made between GSM900 and DCS1800 BTSs, and the efficiency is the same as the single-band inter-BTS handoff [15].

Previous works in [1] and [18] studied the capacity of dual-band systems for Type-II connection by considering separate single-band and dual-band MSs. In these models, single-band MSs only can access a part of radio channels while dual-band MSs can change system during call setup (both for the terminating calls and originating calls). Several channel assignment methods were proposed for such systems that do not support handoff services [1]. The effect of handoff issue was studied by a simulation model in [18]. However, cell residence time distributions (specifically, the effect of their variance) have not been studied in literature. In following sections, we investigate the behavior of dual-band MSs in Type-I and Type-II connections by both analytic and simulation models. The call incompletion probabilities are calculated for Gamma cell residence time distributions. Furthermore, we compare the performances of Type-I connection and Type-II connection.

IV. THE ANALYTIC MODEL

This section proposes an analytic model to investigate the performance of overlap dual-band GSM networks. We assume that the DCS1800 cells (the radio coverages of DCS1800 BTSs) are of the same size as the GSM900 cells. Furthermore, the GSM900 and DCS1800 BTSs are co-sited. This setup is actually exercised in GSM networks in Taiwan. Alternatively, the network can be configured in a microcell/macrocell structure where the number of DCS1800 BTSs is typically 2-4 times as many as that of GSM900 BTSs. The microcell/macrocell structure is out of the scope of this paper, and the reader is referred to [16], [4], [12] for the details.

The following input measures are considered for modeling Type-I connection:

- c_G: the number of radio channels at a GSM900 BTS
- c_D: the number of radio channels at a DCS1800 BTS
- λ_{oGO} (λ_{oDO}): the rate of the call origination attempts that MSs make through a GSM900 (DCS1800) BTS; the call origination arrivals are assumed to be a Poisson process
- λ_{oGT} (λ_{oDT}): the rate of the call termination attempts to a GSM900 (DCS1800) BTS; the call termination arrivals are assumed to be a Poisson process
- $\frac{1}{\mu}$: the mean call holding time; the call holding times have an Exponential density function $f_c(t_c) = \mu e^{-\mu t_c}$
- $\frac{1}{\eta}$: the mean cell residence time of an MS at a BTS; the cell residence time distribution is assumed to be Exponential (this Exponential restriction is relaxed in our simulation model)
- ϑ: the probability that an inter-system handoff fails

For Type-I connection, the output measures considered in our study include

- P_{oGO} (P_{oDO}): the *new call blocking probability* for GSM900 (DCS1800) call origination
- P_{oGT} (P_{oDT}): the new call blocking probability for GSM900 (DCS1800) call termination
- P_o: the new call blocking probability that an arbitrary new call is blocked due to the lack of idle channel, where

$$P_o = \frac{\lambda_{oGO}P_{oGO} + \lambda_{oGT}P_{oGT} + \lambda_{oDO}P_{oDO} + \lambda_{oDT}P_{oDT}}{\lambda_{oGO} + \lambda_{oGT} + \lambda_{oDO} + \lambda_{oDT}}. \tag{1}$$

- $\lambda_{hG}(\lambda_{hD})$: the handoff call arrival rate to a GSM900 (DCS1800) BTS
- P_f: the *force-termination probability* that a handoff request is blocked. We further define $P_{fG}(P_{fD})$ as the force-termination probability for GSM900 (DCS1800) system. The probability P_f can be computed as

$$P_f = \frac{\lambda_{hG}P_{fG} + \lambda_{hD}P_{fD}}{\lambda_{hG} + \lambda_{hD}}. \tag{2}$$

- P_{nc}: the *call incompletion probability* that a call is not complete due to a new call blocking or a force-termination. It can be obtained by Eq. (3) shown at the bottom of this page.

For Type-II connection, there is no need to distinguish call originations from call terminations, and its modeling is the same as that for a single-band GSM network where the number of channels at a BTS is $c_G + c_D$ and the call arrival rate is $\lambda_{oGO} + \lambda_{oGT} + \lambda_{oDO} + \lambda_{oDT}$.

Furthermore, the force-termination probability P_f is the same as the new call blocking probability P_o since the handoff calls and the new calls are not distinguishable in GSM channel assignment. Following the technique we proposed in [10], the Type-II network can be modeled by using the Erlang-B formula and an iterative algorithm that computes the new call blocking probability and the force-termination probability in the steady state. The reader is referred to [10] for the modeling details.

The remainder of this section describes the analytic model for Type-I configuration. In this configuration, originating and handoff calls can be switched from one frequency band to the other if no idle channel is available in the original frequency band. However, the terminating calls can not be switched to the other frequency band as we pointed out in Subsection III-A. We also consider the effect of inter-system handoff failure. If the inter-system handoff time is longer than a timeout period or if the network resources (such as inter-MSC trunk) are not available, the network fails to complete the handoff process.

We analyze the Type-I dual-band GSM network by a two-dimensional Markov process. The state transition diagram is shown in Fig. 5. A state in this process is defined as (i, j), where i $(0 \le i \le c_G)$ is the number of busy channels in GSM900 BTS and j $(0 \le j \le c_D)$ is the number of busy channels in DCS1800 BTS.

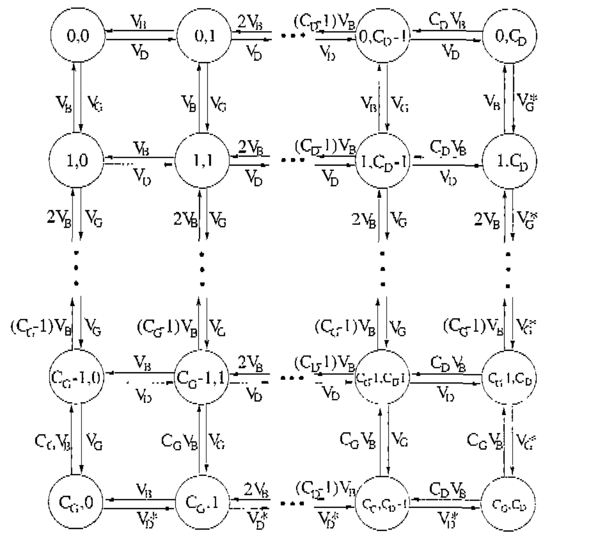

Fig. 5. State transition diagram of the Markov process for Type-I connection.

The transition rates V_G, V_D, V_B, V_G^* and V_D^* used in Fig. 5 are defined as

$$\begin{aligned} V_G &= \lambda_{oGO} + \lambda_{oGT} + \lambda_{hG}, \\ V_D &= \lambda_{oDO} + \lambda_{oDT} + \lambda_{hD}, \\ V_B &= \mu + \eta, \\ V_G^* &= \lambda_{oGO} + \lambda_{oGT} + \lambda_{hG} + \lambda_{oDO} + (1-\vartheta)\lambda_{hD} \\ &= V_G + \lambda_{oDO} + (1-\vartheta)\lambda_{hD}, \\ V_D^* &= \lambda_{oDO} + \lambda_{oDT} + \lambda_{hD} + \lambda_{oGO} + (1-\vartheta)\lambda_{hG} \\ &= V_D + \lambda_{oGO} + (1-\vartheta)\lambda_{hG}. \end{aligned}$$

The transitions of the process are described below.

- For $0 \le i < c_G$ and $0 \le j < c_D$, idle channels in both GSM900 and DCS1800 bands are available at the co-sited BTS. Thus, the process moves from (i,j) to $(i+1,j)$ with rate $V_G = \lambda_{oGO} + \lambda_{oGT} + \lambda_{hG}$, and moves from (i,j) to $(i,j+1)$ with rate $V_D = \lambda_{oDO} + \lambda_{oDT} + \lambda_{hD}$.
- The channel occupation time of a call is the minimum of the remaining call holding time and the remaining cell residence time. Since the call holding times and cell residence times are both exponentially distributed with rate μ and η respectively, the channel occupancy time is also exponentially distributed with rate $V_B = \mu + \eta$. Thus, the process moves from (i,j) to $(i-1,j)$ with rate iV_B for $0 < i \le c_G$. Similarly, the process moves from (i,j) to $(i,j-1)$ with rate jV_B for $0 < j \le c_D$.
- When the process is at state (c_G, j) for $0 \le j < c_D$, all GSM900 channels are busy. For a GSM terminating call arrival, it is dropped. On the other hand, for

$$P_{nc} = \frac{\lambda_{oGO}P_{oGO} + \lambda_{oGT}P_{oGT} + \lambda_{hG}P_{fG} + \lambda_{oDO}P_{oDO} + \lambda_{oDT}P_{oDT} + \lambda_{hD}P_{fD}}{\lambda_{oGO} + \lambda_{oGT} + \lambda_{oDO} + \lambda_{oDT}} \tag{3}$$

an originating call or a handoff request, the MS is asked to re-try the DCS1800 band. In this case, a DCS1800 channel is available and the GSM900 originating call is served (and is turned into a DCS1800 call). However, the handoff request may be dropped if the inter-system handoff time is too long or if network resources are not available (with probability ϑ). Thus, the process moves from (c_G, j) to $(c_G, j+1)$ with rate $V_D^* = \lambda_{oDO} + \lambda_{oDT} + \lambda_{hD} + \lambda_{oGO} + \lambda_{hG}(1-\vartheta)$. Similarly, when the process is in (i, c_D), where $0 \le i < c_G$, the process moves from (i, c_D) to $(i+1, c_D)$ with rate $V_G^* = \lambda_{oGO} + \lambda_{oGT} + \lambda_{hG} + \lambda_{oDO} + \lambda_{hD}(1-\vartheta)$.

Let $p(i,j)$ be the stationary probability for state (i,j), which satisfies the following constraint

$$\sum_{i=0}^{c_G}\sum_{j=0}^{c_D} p(i,j) = 1. \tag{4}$$

The stationary probabilities can be calculated by solving the $(c_G+1)(c_D+1)$ balanced equations and (4). Then the following output measures can be derived by using the stationary probability $p(i,j)$:

- An originating call is blocked if neither a GSM900 channel nor a DCS1800 channel is available at the co-sited BTS. We have

$$P_{oGO} = P_{oDO} = p(c_G, c_D). \tag{5}$$

- Since the terminating calls at one band can not use the radio channels at the other band, we have

$$P_{oGT} = \sum_{0\le i\le c_D} p(c_G, i) \quad \text{and} \quad P_{oDT} = \sum_{0\le i\le c_G} p(i, c_D). \tag{6}$$

- Since the force-termination probability for a GSM900 handoff call is the probability that the call is dropped when no idle radio channel is available in both bands (with probability P_{oGO}) or when no GSM900 channel is available at the new BTS but one or more DCS1800 channels are available and the inter-system handoff fails (with probability $(P_{oGT} - P_{oGO})\vartheta$). Thus, the GSM900 force-termination probability is

$$P_{fG} = P_{oGO} + (P_{oGT} - P_{oGO})\vartheta. \tag{7}$$

Similarly, the DCS1800 force-termination probability is

$$P_{fD} = P_{oDO} + (P_{oDT} - P_{oDO})\vartheta. \tag{8}$$

Let P_{no} be the probability that a new call at the cell is not complete before the MS moves out of the cell (i.e., the new call "overflow" probability), and P_{ho} be the probability that a handoff call at a cell is not complete before the MS moves out of the cell (i.e., the handoff call "overflow" probability). From [10], we have

$$P_{no} = P_{ho} = \frac{\eta}{\mu+\eta}. \tag{9}$$

The GSM900 handoff call arrival rate λ_{hG} is

$$\begin{aligned}\lambda_{hG} &= [\lambda_{hG}(1-P_{oGT}) + \lambda_{hD}(P_{oDT}-P_{oDO})(1-\vartheta)]\,P_{ho}\\ &+ [(\lambda_{oGO}+\lambda_{oGT})(1-P_{oGT})\\ &+ \lambda_{oDO}(P_{oDT}-P_{oDO})]\,P_{no}.\end{aligned} \tag{10}$$

Eq. (10) implies that handoff calls overflow from a co-siting BTS A to A's neighbors in four cases:

- When a handoff call entered BTS A, it was a GSM call and it received a GSM radio channel at BTS A (with rate $\lambda_{hG}(1-P_{oGT})$). The call is not complete at BTS A (with probability P_{ho}).
- When a handoff call entered BTS A, it was a DCS1800 call and it received a GSM radio channel at BTS A (with rate $\lambda_{hD}(P_{oDT}-P_{oDO})(1-\vartheta)$). The call is not complete at BTS A (with probability P_{ho}).
- When a new call entered BTS A, it was a GSM900 call and it received a GSM radio channel at BTS A (with rate $(\lambda_{oGO}+\lambda_{oGT})(1-P_{oGT})$). The call is not complete at BTS A (with probability P_{no}).
- When a new call entered BTS A, it was a DCS1800 call and it received a GSM radio channel at BTS A (with rate $\lambda_{oDO}(P_{oDT}-P_{oDO})$). The call is not complete at BTS A (with probability P_{no}).

From (10), (9) and (7), we have

$$\begin{aligned}\lambda_{hG} &= \frac{\eta}{\mu+\eta P_{oGT}} \times [\lambda_{hD}(P_{oDT}-P_{oDO})(1-\vartheta)\\ &+ (\lambda_{oGO}+\lambda_{oGT})(1-P_{oGT}) + \lambda_{oDO}(P_{oDT}-P_{oDO})].\end{aligned} \tag{11}$$

Similarly, the DCS1800 handoff rate λ_{hD} is:

$$\begin{aligned}\lambda_{hD} &= \frac{\eta}{\mu+\eta P_{oDT}} \times [\lambda_{hG}(P_{oGT}-P_{oGO})(1-\vartheta)\\ &+ (\lambda_{oDO}+\lambda_{oDT})(1-P_{oDT}) + \lambda_{oGO}(P_{oGT}-P_{oGO})].\end{aligned} \tag{12}$$

By using the approach in [10], the following iterative algorithm is executed to compute P_o, P_{fG}, P_{fD}, P_{ncG}, P_{ncD} and P_{nc}:

Step 1. Select initial values for $P_{oGO}, P_{oGT}, P_{oDO}$ and P_{oDT}.

Step 2. Compute handoff rates λ_{hG} and λ_{hD} using (11) and (12).

Step 3. Let $P_{oGO,old} \leftarrow P_{oGO}$, $P_{oGT,old} \leftarrow P_{oGT}$, $P_{oDO,old} \leftarrow P_{oDO}$ and $P_{oDT,old} \leftarrow P_{oDT}$.

Step 4. Compute $P_{oGO}, P_{oGT}, P_{oDO}$ and P_{oDT} by using (5) and (6).

Step 5. Let δ be a pre-defined small value. If $|P_{oGO,old} - P_{oGO}| > \delta P_{oGO}$, $|P_{oGT,old} - P_{oGT}| > \delta P_{oGT}$, $|P_{oDO,old} - P_{oDO}| > \delta P_{oDO}$ or $|P_{oDT,old} - P_{oDT}| > \delta P_{oDT}$, then go to Step 2. Otherwise, go to Step 6.

Step 6. Compute P_o, P_{fG}, P_{fD}, P_f and P_{nc} using (1), (7), (8), (2) and (3), respectively.

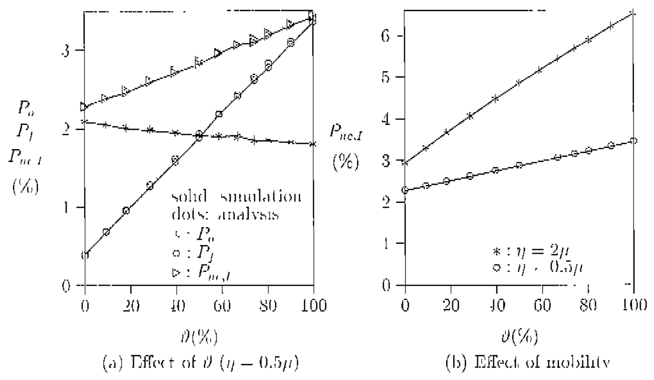

Fig. 6. Effect of inter-system handoff failure rate ($\lambda = 4.5\mu$ and $c_G = c_D = 14$) on Type-I connection.

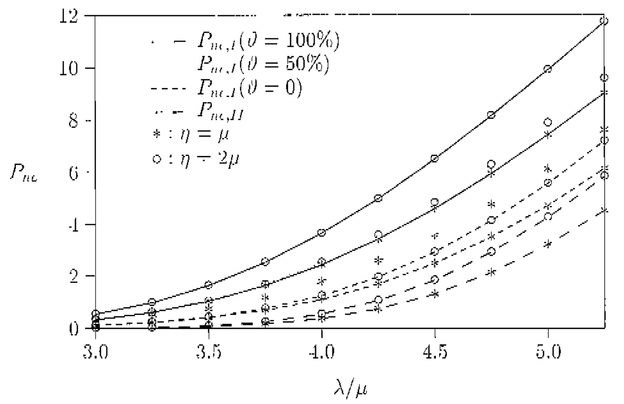

Fig. 7. Effects of η and $\vartheta (c_G = c_D = 14)$.

The above analytic model is validated by simulation experiments. The simulation model is similar to the ones we developed in [5]. Fig. 6 (a) plots the output measures for Type-I connection where $\lambda = \lambda_{oGO} = \lambda_{oGT} = \lambda_{oDO} = \lambda_{oDT}$. The solid curves are for simulation results and the dashed curves are for analytic results. These curves indicate that the analytic results and the simulation results are consistent (for other figures presented in this paper, consistent results for simulation and analysis are also observed).

V. NUMERICAL RESULTS

Based on the model described in the previous section, we study the effects of the input parameters on the new call blocking, the force-termination and the incompletion probabilities.

A. Effect of the Inter-system Handoff Failure Rate

Fig. 6 (a) plots P_o, P_f and P_{nc} as functions of the inter-system handoff failure rate ϑ for Type-I connection, where $\lambda = 4.5\mu$, $\eta = 0.5\mu$ and $c_G = c_D = 14$. We observe that as ϑ increases, P_f and P_{nc} rapidly increase and P_o slowly decreases. Since the handoff calls are more likely to be forced terminated for larger ϑ, the resource released from the force-terminated calls are available to the new calls. Thus, P_o decreases.

Fig. 6 (b) illustrates the call incompletion probability $P_{nc,I}$ for Type-I connection as a function of the inter-system handoff failure rate with different mobility values. We consider the cases where $\eta = 0.5\mu$ and 2μ. The figure shows an intuitive result that as ϑ increases, $P_{nc,I}$ increases more rapidly for the case where $\eta = 2\mu$ than the case where $\eta = 0.5\mu$. That is, the effect of ϑ on P_{nc} is more significant for a large mobility than a small one. Consider the case when $\vartheta = 100\%$. For low mobility (i.e., $\eta = 0.5\mu$), the portion of call incompletion due to inter-system handoff failure is 44.66%. For high mobility (i.e., $\eta = 2\mu$), the portion is 75.26%. This portion is computed as (13) at the bottom of this page, where $(P_{oGT} - P_{oGO})\vartheta$ and $(P_{oDT} - P_{oDO})\vartheta$ are the force-termination probabilities due to inter-system handoff failures (see (7) and (8)). The result indicates that even when MS mobility η is low, reducing inter-system handoff failure rate is still critical to improving the performance for Type-I connection.

Table 1. The carried load when the system is engineered at 2% P_{nc} (Erlang).

mobility	Type-I ($\vartheta = 0$)	Type-I ($\vartheta = 50\%$)	Type-I ($\vartheta = 100\%$)	Type-II
$\eta = \mu$	4.35	4.07	3.87	4.71
$\eta = 2\mu$	4.26	3.85	3.61	4.54

B. Comparison of Type-I and Type-II Connections

This subsection compares Type-I connection with Type-II connection. Fig. 7 plots P_{nc} as a function of λ/μ for Type-I connection (with $\vartheta = 0, 50\%$ and 100%) and Type-II connection, where $\eta = \mu$, 2μ and $c_G = c_D = 14$. Table 1 lists the traffic load carried by Type-I and Type-II connections when the system is engineered at 2% blocking probability (i.e., P_{nc}). In the table, the offered loads are given in Erlang for $\eta = \mu$ and 2μ, $c_G = c_D = 14$ and $\vartheta = 0, 50\%$ and 100%. We observe that for $\eta = \mu$, the improvement of Type-II connection over Type-I connection (i.e., extra workload that Type-II connection can carry over Type-I connection) can be up to 8.28% for $\vartheta = 0$, 15.72% for $\vartheta = 50\%$ and 21.71% for $\vartheta = 100\%$. For $\eta = 2\mu$, the improvement of Type-II connection over Type-I connection can be up to 6.57% for $\vartheta = 0$, 17.92% for $\vartheta = 50\%$ and 25.76% for $\vartheta = 100\%$. We conclude that for both high and low mobilities, Type-II connection significantly outperforms Type-I connection (even when the inter-system handoff failure rate is small).

C. Effect of Originating Call Traffic Ratio

Define the originating call traffic ratio ξ as the ratio of the originating call traffic to the total call traffic. The ratio ξ is about

$$\frac{\lambda_{hG}(P_{oGT} - P_{oGO})\vartheta + \lambda_{hD}(P_{oDT} - P_{oDO})\vartheta}{\lambda_{oGO}P_{oGO} + \lambda_{oGT}P_{oGT} + \lambda_{hG}P_{fG} + \lambda_{oDO}P_{oDO} + \lambda_{oDT}P_{oDT} + \lambda_{hD}P_{fD}} \quad (13)$$

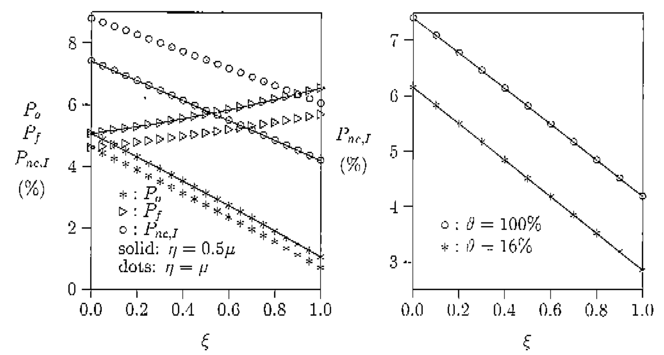

(a) $\vartheta = 100\%$ (b) $\eta = 0.5\mu$

Fig. 8. Effect of originating call traffic ratio ($c_G = c_D = 14$) on Type-I connection.

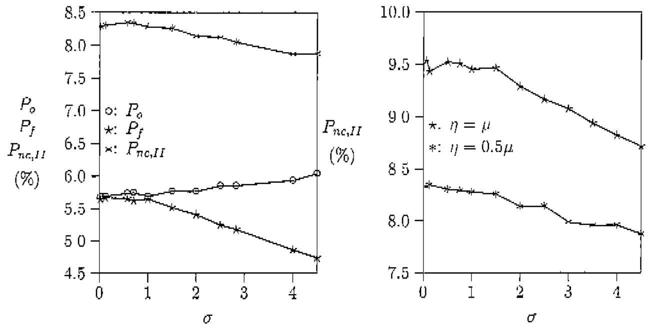

(a) $\eta = 0.5\mu$ (b) Effect of η

Fig. 9. Effects of σ ($c_G = c_D = 14$, $\eta = 0.5\mu$ and $\lambda = 6\mu$) on Type-II connection.

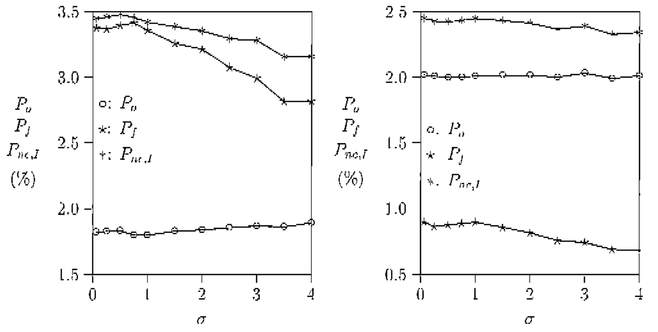

(a) $\vartheta = 100\%$ (b) $\vartheta = 16\%$

Fig. 10. Effect of σ ($c_G = c_D = 14$, $\eta = 0.5\mu$ and $\lambda = 4.5\mu$) on Type-I connection.

40% for a typical GSM system. For a GSM system with pre-paid phone service [2], the ratio is about $10\% - 25\%$. By fixing the total call arrival rate (i.e., $\lambda_{oGO} + \lambda_{oGT} + \lambda_{oDO} + \lambda_{oDT}$) to 20 μ, Fig. 8 (a) plots P_o, P_f and P_{nc} as functions of ξ for Type-I connection. In the figure, $\lambda_{oGO} = \lambda_{oDO} = 10\xi\mu$, $\lambda_{oGT} = \lambda_{oDT} = 10(1-\xi)\mu$ and $c_G = c_D = 14$. We observe that P_o and P_{nc} decrease and P_f increases as ξ increases. Note that the originating calls can switch from one band to the other if no idle radio channel is available in the original band. When the originating call traffic increases, new calls have more opportunities to be accepted. Thus, P_o decreases.

Fig. 8 (b) plots P_{nc} as a function of ξ for $\vartheta = 100\%$ and $\vartheta = 16\%$. As ξ increases, P_{nc} for $\vartheta = 16\%$ decreases more rapidly

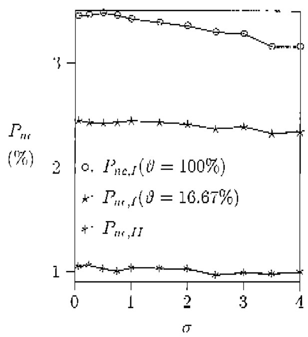

Fig. 11. Comparison of Type-I and Type-II connections ($c_G = c_D = 14$, $\eta = 0.5\mu$ and $\lambda = 4.5\mu$).

than that for $\vartheta = 100\%$. The effect of the originating call traffic ratio on P_{nc} is more significant when the inter-system handoff failure rate is small. The $P_{nc,I}(\vartheta = 100\%)$ to $P_{nc,I}(\vartheta = 16\%)$ ratio at $\xi = 0$ is about 1.20 and the ratio at $\xi = 1$ is about 1.47. The phenomenon suggests that the inter-system handoff failure rate has a more significant effect on P_{nc} for a larger originating call traffic ratio. For a dual-band GSM system without pre-paid service, it is more important to reduce ϑ than that with pre-paid call service.

D. Effect of the Variation of the Cell Residence Times

This subsection studies the effect of the cell residence time distribution based on simulation results. For the demonstration purposes, we use Gamma residence time distribution. The Gamma distribution is selected because it can be shaped to represent many other distributions [6].

A Gamma distribution has the density function

$$f_G(t) = \frac{\beta^\alpha}{\Gamma(\alpha)} t^{\alpha-1} e^{-\beta t} \text{ for } t > 0,$$

where $\alpha > 0$ is the scale parameter, $\beta > 0$ is the shape parameter and $\Gamma(p) = \int_{x=0}^{\infty} x^{p-1} e^{-x} dx$. The mean of the distribution is $1/\eta = \alpha/\beta$ and the variance is α/β^2. With a fixed mean, we study the effect of the coefficient of variation of the Gamma residence time distribution. The coefficient of variation $\sigma = 1/\sqrt{\alpha}$ is the ratio of the standard derivation to the mean, which is an important quantity in statistics and queuing theory [7]. A large σ represents that the cell residence times have a large variance.

Fig. 9 (a) illustrates P_o, P_f and P_{nc} as functions of σ for Type-II connection. In this figure, $c_G = c_D = 14, \eta = 0.5\mu$ and $\lambda = 6\mu$. We observe the following:

- For $\sigma \leq 1$, all performance measures are insensitive to the variance of the cell residence time distribution.
- For $\sigma > 1$, P_o increases and P_{nc} and P_f decrease as σ increases.

Fig. 9 (b) plots P_{nc} as a function of σ for $\eta = 0.5\mu$ and μ. When $\eta = \mu$, as σ increases, P_{nc} decreases more rapidly for the case where $\eta = \mu$ than the case where $\eta = 0.5\mu$. That is, σ has more significant effect on P_{nc} for a larger mobility.

Fig. 10 (a) and (b) illustrate P_o, P_f and P_{nc} as functions of σ for Type-I connection with $\vartheta = 100\%$ and $\vartheta = 16\%$, respectively. We observe that P_f and P_o are no longer the same in Type-I connection.

Fig. 11 plots P_{nc} as a function of σ for Type-I connection (with $\vartheta = 100\%$ and 16.67%, respectively) and Type-II connection, where $c_G = c_D = 14$, $\eta = 0.5\mu$ and $\lambda = 4.5\mu$. The figure indicates P_{nc} increases as σ decreases for Type-I connection. On the other hand, P_{nc} is insensitive to σ for Type-II connection. Thus, traffic engineering for Type-II connection is easier than Type-I connection because the effect of σ can be ignored.

VI. CONCLUSION

This paper studied dual-band GSM network performance. Specifically, we investigated how the radio channel capacities, the inter-system handoff failure rate ϑ, the mobility rate η and the originating call traffic ratio affect the system performance such as call incompletion probability P_{nc}. Our analysis indicates the following.

- The effect of inter-system handoff failure rate ϑ on P_{nc} is more significant for a large mobility η than a small one. The results further indicate that even when MS mobility is low, reducing ϑ is critical to improving the performance for Type-I connection.
- In terms of P_{nc}, the Type-II connection significantly outperforms Type-I connection (even when the inter-system handoff failure rate is small).
- The inter-system handoff failure rate ϑ has significant effect on P_{nc} for large originating call traffic ratio. It is important to reduce ϑ for Type-I connection with heavy originating call traffic.
- P_{nc} decreases as the variance of the cell residence time distribution increases. Specifically, P_{nc} in Type-I connection with a large inter-system handoff failure rate is much more sensitive to the variance than Type-II connection.

ACKNOWLEDGEMENT

We would like to thank the three anonymous reviewers for their valuable comments that significantly improve the quality of this paper. Dr. Youngnam Han's assistance in reviewing this paper is highly appreciated. W.R. Lai and Y.-B. Lin's work was supported in part by National Science Council, R.O.C. Contract number NSC-88-2213-E-009-079. H. Rao's work was supported in part by AT&T Laboratories, U.S.A.

REFERENCES

[1] R. Domingo Lara, Rubén Vázquez M., and David Muñoz R., "Channel assignment in dual cellular systems," in *Proc. of 1993 IEEE Vehicular Technology Conference*, 1993, pp. 198–201.
[2] D. Edwards, "Pay now, call later," *Telecommunications*, Mar. 1998.
[3] ETSI/TC, "Mobile application part (MAP) specification, version 4.8.0," Technical Report Recommendation GSM 09.02, ETSI, 1994.
[4] C.-L. I, L. J. Greenstein, and R. D. Gitlin, "A microcell/macrocell cellular architecture for low and high-mobility wireless users," *IEEE J. Select. Areas Commun.*, vol. 11, no. 6, pp. 885–891, 1993.
[5] J.-Y. Jeng, C.-W. Lin, and Y.-B. Lin, "Dynamic resource scheduling for GSM data services," *IEICE Trans. Commun.*, vol. 80-B, no. 2, pp. 296–300, 1997.
[6] N. L. Johnson, *Continuous Univariate Distributions-1*, John Wiley & Sons, 1970.
[7] L. Kleinrock, *Queueing Systems: Volume I – Theory*, New York: Wiley, 1976.
[8] W. C. Y. Lee, *Mobile Cellular Telecommunications Systems*, McGraw-Hill, 1995.
[9] Y.-B. Lin, "Mobility management for cellular telephony networks," *IEEE Parallel & Distributed Technology*, vol. 4, no. 4, pp. 65–73, Nov. 1996.
[10] Y.-B. Lin, "Performance modeling for mobile telephone networks," *IEEE Network Magazine*, vol. 11, no. 6, pp. 63–68, Nov./Dec. 1997.
[11] Y.-B. Lin and I. Chlamtac, "Heterogeneous personal communications services: Integration of PCS systems," *IEEE Commun. Magazine*, vol. 34, no. 9, pp. 106–113, 1996.
[12] Y.-B. Lin, A. R. Noerpel, and L.-F. Chang, "Modeling hierarchical microcell/macrocell PCS architecture," *IEEE ICC*, 1995.
[13] Mehrotra, *GSM System Engineering*, Artech House, 1997.
[14] M. Mouly and M.-B. Pautet, *The GSM System for Mobile Communications*, M. Mouly, 49 rue Louise Bruneau, Palaiseau, France, 1992.
[15] J. O'Konek, "Dual band network infrastructure," *Technical report*, Far EasTone Telecommunications, Ltd., Taiwan, 1998.
[16] R. A. Ramsdale and W. B. Harrold, "Techniques for cellular networks incorporating microcells," in *Proc. of 2nd International Symposium on Personal, Indoor, and Mobile Radio Commun.*, 1992, pp. 169–173.
[17] S. Redl and M. Weber, *An Introduction to GSM*, Artech House, 1995.
[18] S. Tegler, S. Alexius, P. Lind, and T. Liunggren, "Improving capacity in a GSM system with DCS1800 and dual band mobiles," in *Proc. of Wireless Networks Catching the Mobile Future*, 1994, pp. 1162–1166.

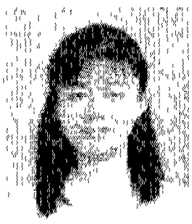

Wai-Ru Lai is a graduate student of the Department of Computer Science and Information Engineering, National Chiao Tung University. Her current research interests include design and analysis of personal communications services network.

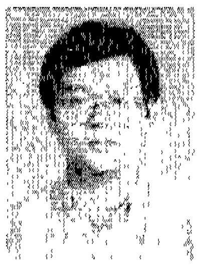

Yi-Bing Lin received his BSEE degree from National Cheng Kung University in 1983, and his Ph.D. degree in Computer Science from the University of Washington in 1990. From 1990 to 1995, he was with the Applied Research Area at Bell Communications Research (Bellcore), Morristown, NJ. In 1995, he was appointed as a professor of Department of Computer Science and Information Engineering (CSIE), National Chiao Tung University (NCTU). In 1996, he was appointed as Deputy Director of Microelectronics and Information Systems Research Center, NCTU. In 1997, he was elected as Chairman of CSIE, NCTU. His current research interests include design and analysis of personal communications services network, mobile computing, distributed simulation, and performance modeling.

Dr. Lin is a subject area editor of the Journal of Parallel and Distributed Computing, an associate editor of the International Journal in Computer Simulation, an associate editor of IEEE Network, an editor of the ACM/Baltzer WINET, an associate editor of SIMULATION magazine, an area editor of ACM Mobile Computing and Communication Review, a columnist of ACM Simulation Digest, a member of the editorial board of International Journal of Communications Systems, a member of the editorial board of Computer Simulation Modeling and Analysis, Program Chair for the 8th Workshop on Distributed and Parallel Simulation, General Chair for the 9th Workshop on Distributed and Parallel Simulation, Program Chair for the 2nd International Mobile Computing Conference, the publicity chair of ACM Sigmobile, Guest Editor for the ACM/Baltzer MONET special issue on Personal Communications, and Guest Editor for IEEE Transactions on Computers special issue on Mobile Computing. Dr. Lin is a senior member of IEEE. Lin's email address is liny@csie.nctu.edu.tw.

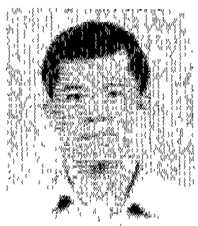

Herman Chung-Hwa Rao is a Principal Technical Staff in ATT Laboratories-Research. His research interests are in the area of Internet, Distributed File Systems, Distributed Systems, Mobile Computing, Operating Systems, Computer Networks, and Software Tools. In particular, he has been involved in the design and implementation of an Internet File System, Middleware for Web Client, and GRADIENT (Global Research And Development envIronmENT). He received his Ph.D. and M.S. in Computer Science from the University of Arizona and his B.S. in Mechanical Engineering from the National Taiwan University.